Published in final edited form as:

Muscle Nerve. 2019 February ; 59(2): 254–262. doi:10.1002/mus.26365.

Muscle contractility dysfunction precedes loss of motor unit connectivity in SOD1(G93A) mice

Christopher G. Wier, BS[1], **Alexander E. Crum**[2], **Anthony B. Reynolds, BA**[1], **Chitra C. Iyer, PhD**[2], **Deepti Chugh, PhD**[2], **Marilly S. Palettas, BS**[3], **Patrick L. Heilman, PhD**[2], **David M. Kline, PhD**[3], **W. David Arnold, MD**[2,4,5,6], and **Stephen J. Kolb, MD, PhD**[1,2]

[1]Department of Biological Chemistry and Pharmacology, The Ohio State University Wexner Medical Center

[2]Department of Neurology, The Ohio State University Wexner Medical Center

[3]Center for Biostatistics, Department of Biomedical Informatics, The Ohio State University, Columbus, OH

[4]Department of Physical Medicine and Rehabilitation, The Ohio State University Wexner Medical Center

[5]Department of Neuroscience, The Ohio State University Wexner Medical Center

[6]Department of Physiology and Cell Biology, The Ohio State University Wexner Medical Center

Abstract

Introduction: Electrophysiological measurements are used in longitudinal clinical studies to provide insight into the progression of amyotrophic lateral sclerosis (ALS) and the relationship between muscle weakness and motor unit degeneration. Here, we used a similar longitudinal approach in the SOD1(G93A) mouse model of ALS.

Methods: *In vivo* muscle contractility and motor unit connectivity assays were assessed longitudinally in SOD1(G93A) and wildtype mice from post-natal day 35 to 119.

Results: In SOD1(G93A) males, muscle contractility was reduced by day 35 and preceded motor unit loss. Muscle contractility and motor unit reduction were delayed in SOD1(G93A) females when compared with males, but as with males, muscle contractility reduction preceded motor unit loss.

Discussion: The longitudinal contractility and connectivity paradigm employed here provides additional insight into the SOD1(G93A) mouse model and suggests that loss of muscle contractility is an early finding that may precede loss of motor units and motor neuron death.

Corresponding Author: W. David Arnold, M.D., Department of Neurology, Division of Neuromuscular Medicine, The Ohio State University Wexner Medical Center, 395 W. 12th Ave, Columbus, OH 43210, USA, William.arnold@osumc.edu.

Ethical Publication Statement:
We confirm that we have read the Journal's position on issues involved in ethical publication and affirm that this report is consistent with those guidelines

Disclosure of Conflicts of Interest:
None of the authors has any conflict of interest to disclose

Keywords

ALS; Motor unit; Electrophysiology; Connectivity; Contractility

Introduction

Amyotrophic lateral sclerosis (ALS) is a neurodegenerative disorder affecting approximately 5 in 100,000 individuals [1, 2]. The disease is characterized by progressive loss of upper and lower motor neurons resulting in weakness, muscle denervation and atrophy, and eventual death, typically within 3–5 years of symptom onset.

Electrophysiological measures, including compound muscle action potential (CMAP) and motor unit number estimate (MUNE), allow *in vivo* assessment of the motor unit (MU) connectivity. Such measurements have been applied in clinical natural history studies of ALS to provide important insight into the interrelationship of muscle function and MU connectivity [3–7]. A powerful aspect of CMAP and MUNE measurements is that the functional status of the neuromuscular system can be tracked longitudinally to identify disease onset, severity, and rate of progression. Furthermore, MUNE can assess the response of the neuromuscular system to a therapeutic intervention, from the standpoint of preservation or regeneration of MU number as well as increased output from individual MUs (i.e., compensatory collateral reinnervation) [8–10]. As such, a number of clinical studies have leveraged electrophysiological measures to gain pathophysiological insight into longitudinal disease progression, including the timing and rate of MU loss, the ability of individual MUs to develop collateral sprouting, and the relationship between MU degeneration and onset of muscle weakness [4, 7, 11–13]. Dantes and McComas demonstrated ~50% losses of MUs six months after initial screening, followed by a rapid reduction in MUNE over one year—nearly halving every six months—before reduction slowed over the next 18 months [4]. This study also demonstrated a corresponding increase in the single motor unit potential (SMUP) amplitude, consistent with reinnervation by collateral axonal sprouting of surviving MUs—probably explaining why patients might present with absent or mild muscle weakness despite such a dramatic reduction in MUNE. Another early clinical study by Yuen and Olney measured CMAP and MUNE in addition to functional grip strength in ten ALS patients over the course of six months [7]. They reported a significant reduction in MUNE at three and six months after initial screening and single fiber EMG demonstrated increased mean fiber density of the abductor digiti minimi. During this time CMAP and grip strength did not reduce, which the authors argued as evidence for the compensatory ability of remaining motor neurons via collateral sprouting. Clinical studies that track the natural history of MU integrity during ALS, like the aforementioned, provide several useful insights, including potential treatment windows and underlying dynamic biological processes that could not otherwise be studied [14–17].

Overexpression of human SOD1 with a G93A mutation was used to develop the first mouse model of ALS in 1994 [18, 19]. A number of studies have investigated neuromuscular function in the SOD1(G93A) mouse model using either electrophysiological or physiological measures, [20–32]. Of particular interest are several cross-sectional disease

progression studies of MU dysfunction [21–23, 32]. Hegedus and colleagues demonstrated fast-twitch MU loss as early as post-natal day 40 (P40) utilizing *in situ* muscle contractile measurements [21]. Mancuso and colleagues also demonstrated pre-symptomatic CMAP amplitude reduction by P56 [32]. One of the challenges to understanding the pre-symptomatic changes that occur in the MU has been the difficulty of following the relationships between physiological (muscle contractility; twitch torque and tetanic torque) and electrophysiological (MU connectivity; CMAP and MUNE) measures in individual animals over the course of the disease in a way that mimics the longitudinal clinical studies performed in humans. We have recently applied methodology to perform *in vivo* longitudinal assessments in mouse models of neuropathy [33], spinal muscular atrophy [34, 35], and aging [36] and, here, have applied these methods to the SOD1(G93A) mouse.

Materials and methods

Animals

All procedures were performed in accordance with NIH Guidelines and approved by the Institutional Animal Care and Use Committee (IACUC) of the Ohio State University. A total of 54 mice were used in this study for reliability testing and for the longitudinal analysis of disease progression in the SOD1(G93A) mouse model. Adult wildtype and SOD1(G93A) (C57BL/6xSJL/J; No: 002726) mice used for longitudinal studies and pathology were obtained from Jackson Laboratories (Bar Harbor, ME). Wildtype C57BL/6 mice used for intra-rater reliability testing were obtained from Taconic Biosciences (Albany, NY). All procedures were performed with blinded raters.

Procedures

Behavioral assessments.—Body weight was recorded prior to performing grip strength and rotarod [37, 38]. For grip strength, the average right hindlimb grip strength, measured in grams, was calculated from five measurements per assessment using a standard grip meter (DEFII-002, Chatillon, Largo, FL, USA). Mice were positioned to allow only the right hindpaw to grasp the grid and were pulled towards the evaluator for the length of the grip meter [39]. Attempts that were ≥ ±10g different than the other attempts were discarded and re-performed. The average of three motor coordination tests was measured using an accelerating rotarod (LE8205, Panlab Harvard Apparatus) starting at 5RPM. Trials were stopped if 120s passed without a fall.

Anesthesia and animal preparation.—Mice were anesthetized (isoflurane inhalation, 1.5–3%) during electrophysiological and muscle physiological recordings. Lubricant ointment was applied to the eyes to prevent corneal drying. All measurements were performed on the right hindlimb which was shaved with electric clippers prior to studies. Electrophysiological procedures were performed on a heated platform set at 37°C (World Precision Instruments, Sarasota, FL). During muscle contractility procedures, a warm water bath HTP-1500 Heat Therapy Pump set at 37°C was used to maintain temperature of the testing stage (Androit Medical Systems, Loudon, TN). Procedures under anesthesia were typically less than 20 minutes.

Electrophysiology.—CMAP and MUNE were recorded as previously described [34, 35, 40]. Briefly, an active ring electrode was placed superficially over the right triceps surae (gastrocnemius and soleus) and a reference ring electrode was placed superficially over the metatarsals of the right hindpaw (Alpine Biomed, Skovlunde, Denmark). A ground electrode was placed on the tail (Carefusion, Middleton, WI). The sciatic nerve was stimulated (0.1ms pulse, 1–10mA intensity) using two insulated monopolar needles (28G) (Teca, Oxford Instruments Medical, NY). CMAP amplitudes were recorded following supramaximal stimulation (20mV sensitivity, 10Hz low filter, 10kHz high filter). Baseline-to-peak amplitudes were used for comparison of CMAP amplitudes and peak-to-peak amplitudes were used for calculation of MUNE. SMUP was calculated by taking the average of 10 incremental submaximal responses (50μV-500μV sensitivity, 10Hz low filter, 10kHz high filter). MUNE was calculated by dividing the average SMUP amplitude (peak-to-peak) into the maximum peak-to-peak CMAP amplitude. Single fiber electromyography (SFEMG) was recorded, as previously described, in a separate cohort of SOD1(G93A) males (n=3 animals, 19 single muscle fiber action potentials) and wildtype males (n=3 animals, 13 single muscle fiber action potentials) at P35 [41].

Muscle contractility.—Following electrophysiological recordings, mice underwent triceps surae plantarflexion torque assessment using an *in vivo* muscle contractility apparatus (Model 1300A, Aurora Scientific Inc, Canada) (Supplemental Figure 1 and Supplemental Methods) as previously detailed [36]. Briefly, the right hindpaw was taped to the force sensor and positioned at 90°. The hindlimb was extended to position the knee in the locking position and secured at the femoral condyles. Two disposable monopolar electrodes were inserted near the tibial nerve, just posterior to the knee (Natus Neurology, Inc, Middleton, WI). Maximum plantarflexion twitch torque was recorded following a single, supramaximal stimulation (200μs square wave pulse). Maximum tetanic contraction torque was assessed following a train of supramaximal square wave stimulations at 200μs duration delivered at 125Hz stimulation frequency.

NMJ imaging and quantification.—To investigate the morphological correlates of loss of muscle contractility and reduced MU connectivity, the soleus muscle was collected from a separate cohort of SOD1(G93A) (3 males/3 females) and wildtype (3 males/3 females) mice for endpoint studies at P70 and fixed in 4% paraformaldehyde (PFA) at room temperature (RT) for 30min [42, 43]. Muscles were teased into fibers using size 55 forceps (Fine Science Tools) then incubated in blocking buffer (10% goat serum/4% BSA/3% triton-X 100/PBS) at RT for 2hr. An overnight (O/N) primary antibody (α-NF-200, Abcam, Ab72996, [1:5,000]) incubation at 4°C was performed followed by three 10min washes with PBS before receiving a 2hr incubation with secondary antibody (Alex 594 goat α-Chicken, Life Technologies, A11042, [1:1,000]) and α-α-Bungarotoxin-488 (Life Technologies, B13422, [1:1,000]) at RT. Samples then underwent three 10min washes with PBS at RT before being mounted onto Superfrost positively charged glass slides (Fisher Scientific) and sealed using Fluoromount-G (Southern Biotech). Samples were imaged at 20x and 40x magnification using a Leica confocal microscope (Leica DM IRE2) with Leica software (version 2.1). Images were viewed in FIJI (LOCI, University of Wisconsin-Madison) to quantify NMJ

innervation, the co-labeling of NF-200 and α-Bungarotoxin. 95–120 NMJs per muscle sample (per mouse) were scored as fully innervated, partially innervated or denervated.

Experiments:

Intra-rater testing.—Intra-rater reliability was assessed for electrophysiology and muscle contractility. Sixteen wildtype mice (C57BL/6J; 7 males and 9 females) were assessed by an observer (CGW), with one day between trials. Reliability was reported using the intra-class correlation coefficient (ICC), which was defined as poor (ICC≤0.5), moderate (0.5<ICC≤0.75), good (0.75<ICC≤0.9) or excellent (ICC>0.9) [44].

Assessment of longitudinal SOD1(G93A) disease progression.—Raters (AEC, ABR) performed behavioral assessments weekly from P35 to P119 in a total of 20 mice [5 male/5female wildtype (C57BL/6J) and 5 male/5 female SOD1(G93A) (C57BL/6xSJL/J)]. Mice that displayed loss of the righting reflex for 30 seconds were euthanized for tissue harvesting and muscle wet weight recording [45]. Additional SOD1(G93A) (n=6) and wildtype (n=6) mice were sacrificed at P70, and right triceps surae muscles were collected, weighed and processed for NMJ quantification. A single evaluator (CGW) performed the longitudinal electrophysiological and muscle contractility.

Statistics

Intra-rater variability analyses were used to assess the degree of agreement between the electrophysiology and muscle contractility across all mice, over time. The R package irr (R version 3.3.2, The R Foundation for Statistical Computing) was used to perform these analyses.

A mixed effects model was used to model the mean of each of the six outcome variables for the longitudinal experiments. Fixed effects were included for the two groups, SOD1 mutants and wild type, and gender. A random intercept was used to account for repeated measures within mouse. Backward selection was used starting from an initial model with up to 3-way interactions. A square root transformation was used for CMAP, SMUP and MUNE. Furthermore, a quadratic time trend was included for CMAP, MUNE, and normalized twitch torque. Group means were compared at each time point at the 0.05 level using Holm's Method to adjust for multiplicity within each outcome [46]. When group effects differed significantly by gender, comparisons were made within each gender. SAS 9.4 (Cary, NC) was used for the analysis. Unpaired t-test was performed using Graphpad Prism software (version 6) to compare jitter, muscle weight and NMJ quantification. Pearson's correlation coefficients were calculated to determine correlations between: muscle contractility and MU connectivity, behavioral measurements and muscle contractility, and behavioral measurements and MU connectivity. Correlation coefficient strengths were interpreted using prior guidelines, negligible (0.0≤r≤0.3), weak (0.3<r≤0.5), moderate (0.5<r≤0.7), strong (0.7<r≤0.9) and very strong (0.9<r≤1.0) [47]. Statistical significance was set at $p<0.05$.

Results

Intra-rater reliability of CMAP, twitch torque and tetanic torque

CMAP and twitch measurements were moderately reliable with ICCs of 0.62 and 0.68, respectively, while tetanic measurements demonstrated good reliability with an ICC of 0.81.

Reduction of muscle contractility and of motor unit connectivity are early features in SOD1(G93A) mice

Muscle contractility and MU connectivity were assessed longitudinally from P35 to P119 in SOD1(G93A) (5 males/5 females) and wildtype (5 males/5 females) mice (Tables 1 and 2).

Mixed effects models for longitudinal muscle contractility and MU connectivity reduction were used from age P35 to P119 in separate cohorts of male and female mice (Figure 1 and Figure 2, Supplemental tables 1 and 2). Reduced muscle contractility preceded MU connectivity reduction in both male and female SOD1(G93A) mice. Normalized twitch torque in SOD1(G93A) males (0.087mN-m/g, 95% CI: 0.073–0.101mN-m/g) was reduced compared to wildtype males (0.117mN-m/g, 95% CI: 0.103–0.131mN-m/g) at the start of the study (P35) (Figure 1A). Normalized tetanic torque was also reduced at P35 in SOD1(G93A) males (0.48mN-m/g, 95% CI: 0.42–0.54mN-m/g) compared to wildtype males (0.59mN-m/g, 95% CI:0.53–0.65mN-m/g) (Figure 1B). Normalized twitch torque was reduced at P63 in SOD1(G93A) female mice (0.099mN-m/g, 95% CI: 0.088–0.111mN-m/g) compared to wildtype female mice (0.121mN-m/g, 95% CI: 0.110–0.132mN-m/g), whereas normalized tetanic torque was reduced by P56 in SOD1(G03A) females (0.45mN-m/g, 95% CI: 0.41–0.50mN-m/g) relative to wildtype females (0.54mN-m/g, 95% CI: 0.49–0.58mN-m/g) (Figure 1A-B).

CMAP reduction occurred at P42 in SOD1(G93A) males (31.0mV, 95% CI: 25.4–37.2mV) compared to wildtype male mice (44.6mV, 95% CI: 37.8–51.9mV) and at P91 in SOD1(G93A) females (25.7mV, 95% CI: 21.1–30.8mV) compared to wildtype females (39.2mV, 95% CI: 33.4–45.5mV) (Figure 2A). MUNE reduction in SOD1(G93A) males (252, 95% CI: 205–304) relative to wildtype males 368, 95% CI: 310–430) occurred at P49 and at P77 in SOD1(G93A) females (205, 95% CI: 164–251) compared to wildtype females (323, 95% CI: 271–381) (Figure 2B). There was no observed sexual dimorphism in SMUP, with increases occurring at P70 for both SOD1(G93A) males and females (252.0μV, 95% CI: 236.6–267.9μV) relative to wildtype males and females (218.7μV, 95% CI: 204.3–233.5μV) (Figure 2C). Single fiber electromyography (SFEMG) was performed to exclude the possibility that failure of NMJ transmission could be the explanation for early contractility reduction in SOD1 mice. Separate cohorts of SOD1(G93A) males and wildtype males were studied with SFEMG in the gastrocnemius at P35 to assess NMJ integrity. There was no difference in jitter between SOD1(G93A) males (8.02±2.29μs; range: 4.01–12.27μs and wildtype males (8.38±2.45μs; range 5.07–12.57μs) (p=0.669). Table 3 summarizes and compares onset of MU degeneration and reduced muscle contractility.

Muscle atrophy occurs after loss of muscle contractility

We assessed wet triceps surae muscle mass (normalized to body mass) to examine whether the early findings of reduced muscle contractility and loss of MU connectivity were associated with coexistent loss of muscle mass. Separate groups of wildtype and SOD1(G93A) were sacrificed at P70, in addition to the longitudinal cohorts at P119, and their right triceps surae muscles were harvested and weighed (Figure 3). There was no change in the relative percentage of denervated soleus NMJs between SOD1(G93A) and wildtype mice at P70 (Supplemental Figure 2). Despite reduction of both muscle contractility and MU connectivity there were no overt differences in normalized triceps surae wet mass at P70 between wildtype and SOD1(G93A) mice (Figure 3A). At P119, normalized triceps surae wet mass was reduced in SOD1(G93A) mice compared to wildtype mice (Figure 3A). When we organized normalized triceps surae wet mass by sex at P70, there was no difference in normalized triceps surae mass between SOD1(G93A) males relative to wildtype males nor was there difference between SOD1(G93A) female and wildtype female (Figure 3B). At P119, normalized triceps surae mass was reduced in SOD1(G93A) males compared to wildtype males as well as in SOD1(G93A) females compared to wildtype females (Figure 3B).

Correlations between MU connectivity, muscle contractility, and behavioral assessments

Correlations were analyzed between electrophysiological measures, muscle contractility, and grip strength at week 15. MUNE showed a very strong positive correlation with absolute twitch torque and absolute tetanic torque (Figure 4A and 4C), but MUNE showed no significant correlation with normalized twitch and tetanic torque (Figure 4B and 4D). CMAP demonstrated a strong positive correlation with both absolute twitch torque ($r=0.84$, $p<0.01$) and absolute tetanic torque ($r=0.76$, $p<0.05$) and moderately positive correlated with both normalized twitch torque ($r=0.68$, $p<0.05$) and normalized tetanic torque ($r=0.65$, $p<0.05$) (not shown). Grip strength was strongly correlated with CMAP ($r=0.82$, $p<0.01$) and MUNE ($r=0.71$, $p<0.05$) and moderately correlated with absolute twitch torque ($r=0.66$, $p<0.05$) (not shown). There was no significant correlation for grip compared with absolute tetanic torque ($r=0.579$, $p=0.079$), normalized twitch torque ($r=0.513$, $p=0.130$) and normalized tetanic torque ($r=0.516$, $p=0.127$) (not shown).

Discussion

In the SOD1(G93A) mouse model, overt behavioral disease onset is typically observed at approximately P90 [18, 48]. However, behavioral measurements used in SOD1(G93A) mice are limited in their ability to directly and accurately measure MU integrity. A number of physiological and pathological cross-sectional studies that directly assess the MU demonstrated earlier phenotypic features relative to typical behavioral disease onset [20, 21, 23, 32, 49]. Fast fatigable muscles have increased vulnerability to denervation and are less efficient at maintaining NMJ collateral reinnervation [49]. Accordingly, *in situ* contractility analyses of isolated fast fatigable muscles by Hegedus and colleagues demonstrated MU loss and corresponding contractile weakness in male mice as early as P40 [21]. Similarly, our results identified reduction of muscle contractility as early as P35 using non-invasive muscle contractility measurements. In contrast to prior studies, muscle contractility was assessed in

the intact triceps surae muscle, which includes the gastrocnemius, a muscle predominantly comprised of fast-fatigable muscle fibers, and the soleus, predominantly composed of slow-fatigue resistant muscle fibers. Using intact muscle groups with mixed muscle fiber types closely mirrors clinical muscle testing in patients in which multiple muscles are tested together [50].

Our results show that reduced contractility occurs before reduction of MU connectivity in both SOD1(G93A) males and females. Importantly, *in vivo* muscle contractility measurements require intact and functioning motor axons, neuromuscular junctions and muscle excitability contraction coupling. Therefore, it was important to consider whether early NMJ degeneration might explain early twitch and tetanic muscle contraction torque losses. We found several results in our study arguing against this possibility. First, we assessed NMJ transmission using SFEMG which is the most sensitive measure of NMJ transmission *in vivo* [41]. SFEMG at P35 (when the twitch and tetanic muscle contractions were reduced) was unchanged in mutant versus wildtype male mice. Furthermore, twitch and CMAP responses are both measured following a single supramaximal nerve stimulation, and our results showed that reduced twitch occurred prior to CMAP was reduced in both SOD1(G93A) males and females by 7 days and 28 days respectively. Together, the discrepant twitch and CMAP findings, along with our SFEMG results, support excitation-contraction decoupling, and not NMJ transmission failure, as the cause of early contractility reduction. Lastly, if muscle contractility precedes MU connectivity reduction, we would expect to also see no muscle atrophy related to denervation. In our studies, wet muscle weight did not reveal triceps surae (gastrocnemius and soleus) atrophy at P70 when muscle contractility was already reduced, suggesting that loss of muscle contractility was not simply related to muscle size.

Our findings of early reduction of muscle contractility (prior to SFEMG abnormalities and CMAP and MUNE reduction) suggest early subsarcolemmal abnormalities resulting in excitation-contraction decoupling. Prior studies have suggested muscle specific defects in ALS patients and SOD1(G93A) mice [51–54]. Increased oxidative stress in the sarcolemma and the sarcoplasmic reticulum have also been observed in SOD1(G93A) mice [54, 55]. The increased oxidative stress may result in muscle excitation-contraction decoupling, possibly through abnormalities of calcium regulation, myofilament function or ATP production [55, 56]. One protein critical for excitation-contraction coupling which may be negatively impacted to produce early contractile reduction is sarcoplasmic reticulum Ca^{2+} ATPase (SERCA). SERCA pump activity is diminished following increased oxidative stress, with the intracellular Ca^{2+} imbalances resulting in muscle contractile weakness [57, 58].

Sexual dimorphism observed in our studies is consistent with previous reports that SOD1(G93A) males exhibit earlier disease onset compared to their female counterparts in C57BL/6xSJL/J mice [59, 60]. Sex differences appear to be background strain specific. Male SOD1(G93A) mice on the strain used in this work (C57BL/6xSJL/J) as well as SJL have been shown to present earlier symptom onset compared to females, whereas male SOD1(G93A) on C57BL/6 exhibit no sexual differences [59]. A previous study utilized mice generated from SOD1(G93A) C57BL/6xSJL/6 crossed with wildtype C57BL/6 mice and demonstrated no sex-specific differences in MU number loss or in muscle contractile

force deficits [22]. The potential differences in the background strains of SOD1(G93A) mice used may account for the discrepant results.

Our paradigm is strengthened by the capacity for repeat measures of muscle contractility and MU connectivity in individual animals. Previous studies of MU reduction in SOD1(G93A) mice were performed via a cross-sectional paradigm [21–23, 32]. While such cross-sectional analyses allow examination of aggregate differences over time, these do not permit consideration of disease trajectories of individual mice. Utilizing a longitudinal approach allowed us to assess disease progression in individual mice over time and legitimize the approach to use statistical modeling of the disease time course to properly account for heterogeneity between mice. Our results suggest that longitudinal assessments of *in vivo* muscle contractility in conjunction with MU connectivity may be a powerful readout for pre-clinical drug testing in this model as well as other models of neuromuscular disease.

The development of meaningful outcome measures for ALS is critically important. The methodology for measuring muscle contractility presented herein as a physiological outcome measure shares qualities of a good physiological biomarker, in that it is reproducible, minimally-invasive, easy to obtain and has the capacity to make longitudinal measures [61]. Rater reliability results are in line with intra-rater reliabilities of muscle function and MU connectivity measurements in clinical studies (ICCs ranging from 0.55 to 0.99) [62–67] and pre-clinical studies utilizing MU connectivity measurements in mice (ICCs ranging from 0.56 to 0.76) [68]. Muscle contractility measurements following nerve stimulation could be performed alongside current strength tests in people with ALS, such as hand-held dynamometers, with the added benefit of not being impacted by the strength of the evaluator [69].

In conclusion, when combined with longitudinal MU connectivity measurements, muscle contractility measurements allow a more complete analysis of MU innervation and functional status in degenerative models. Early muscle contractility dysfunction occurred prior to MU connectivity deficits and may precede neuronal death in SOD1(G93A) mice. Thus, the design and execution of pre-clinical studies using SOD1(G93A) mice can be enhanced through this paradigm. Moreover, we believe that muscle contractility outcome measures have the potential to be directly applied in patients to detect early changes in contractility.

Supplementary Material

Refer to Web version on PubMed Central for supplementary material.

Acknowledgements:

We would like to thank the Neuroscience Imaging Core at Ohio State University and Paula Monsma for their technical expertise in acquiring NMJ images. We would also like to thank Matthew Borkowski and the technical support staff at Aurora Scientific, Inc for their assistance in setting up the muscle contractility rig.

This project was funded by the National Institutes of Health/National Institute on Aging [R03AG050877], The Neurological Research Institute at The Ohio State Wexner Medical Center, the Julie Bonasera Fund for ALS and Neuromuscular Diseases and the Fred F. and Herman M. Dreier ALS Fund.

Abbreviations:

ALS	amyotrophic lateral sclerosis
CMAP	compound muscle action potentia
ICC	intra-class coefficient
MU	motor unit
MUNE	motor unit number estimation
O/N	overnight
PFA	paraformaldehyde
RT	room temperature
SFEMG	single fiber electromyography
SMUP	single motor unit potential
SOD1	Cu/Zn superoxide dismutase

References

1. Al-Chalabi A and Hardiman O, The epidemiology of ALS: a conspiracy of genes, environment and time. Nat Rev Neurol, 2013 9(11): p. 617–28. [PubMed: 24126629]
2. Talbot K, Clinical tool for predicting survival in ALS: do we need one? J Neurol Neurosurg Psychiatry, 2016 87(12): p. 1275. [PubMed: 27378084]
3. Arasaki K, et al., Longitudinal study of functional spinal alpha motor neuron loss in amyotrophic lateral sclerosis. Muscle Nerve, 2002 25(4): p. 520–6. [PubMed: 11932969]
4. Dantes M and McComas A, The extent and time course of motoneuron involvement in amyotrophic lateral sclerosis. Muscle Nerve, 1991 14(5): p. 416–21. [PubMed: 1870632]
5. Felice KJ, Thenar Motor Unit Number Estimates Using the Multiple Point Stimulation Technique - Reproducibility Studies in Als Patients and Normal Subjects. Muscle & Nerve, 1995 18(12): p. 1412–1416. [PubMed: 7477064]
6. Kelly JJ, Jr., et al., Use of electrophysiologic tests to measure disease progression in ALS therapeutic trials. Muscle Nerve, 1990 13(6): p. 471–9. [PubMed: 2195338]
7. Yuen EC and Olney RK, Longitudinal study of fiber density and motor unit number estimate in patients with amyotrophic lateral sclerosis. Neurology, 1997 49(2): p. 573–8. [PubMed: 9270599]
8. Gooch CL, The canaries in the coal mine: mune and munix in amyotrophic lateral sclerosis. Muscle Nerve, 2017 56(2): p. 183–184. [PubMed: 28445922]
9. Gooch CL, et al., Motor unit number estimation: a technology and literature review. Muscle Nerve, 2014 50(6): p. 884–93. [PubMed: 25186553]
10. Gooch CL and Shefner JM, ALS surrogate markers. MUNE. Amyotroph Lateral Scler Other Motor Neuron Disord, 2004 5 Suppl 1: p. 104–7. [PubMed: 15512887]
11. Armon C and Brandstater ME, Motor unit number estimate-based rates of progression of ALS predict patient survival. Muscle Nerve, 1999 22(11): p. 1571–5. [PubMed: 10514236]
12. Carleton SA and Brown WF, Changes in motor unit populations in motor neurone disease. J Neurol Neurosurg Psychiatry, 1979 42(1): p. 42–51. [PubMed: 216781]
13. Hansen S and Ballantyne JP, A quantitative electrophysiological study of motor neurone disease. J Neurol Neurosurg Psychiatry, 1978 41(9): p. 773–83. [PubMed: 690647]

14. Rutkove SB, Clinical Measures of Disease Progression in Amyotrophic Lateral Sclerosis. Neurotherapeutics, 2015 12(2): p. 384–93. [PubMed: 25582382]
15. Shefner JM, et al., Quantitative strength testing in ALS clinical trials. Neurology, 2016 87(6): p. 617–24. [PubMed: 27385750]
16. Simon NG, et al., Quantifying disease progression in amyotrophic lateral sclerosis. Ann Neurol, 2014 76(5): p. 643–57. [PubMed: 25223628]
17. van Eijk RPA, et al., Monitoring disease progression with plasma creatinine in amyotrophic lateral sclerosis clinical trials. J Neurol Neurosurg Psychiatry, 2018 89(2): p. 156–161. [PubMed: 29084868]
18. Gurney ME, Transgenic-mouse model of amyotrophic lateral sclerosis. N Engl J Med, 1994 331(25): p. 1721–2. [PubMed: 7832899]
19. Zou ZY, et al., Genetic epidemiology of amyotrophic lateral sclerosis: a systematic review and meta-analysis. J Neurol Neurosurg Psychiatry, 2017 88(7): p. 540–549. [PubMed: 28057713]
20. Dibaj P, Schomburg ED, and Steffens H, Contractile characteristics of gastrocnemius-soleus muscle in the SOD1G93A ALS mouse model. Neurol Res, 2015 37(8): p. 693–702. [PubMed: 25917373]
21. Hegedus J, Putman CT, and Gordon T, Time course of preferential motor unit loss in the SOD1 G93A mouse model of amyotrophic lateral sclerosis. Neurobiol Dis, 2007 28(2): p. 154–64. [PubMed: 17766128]
22. Hegedus J, Putman CT, and Gordon T, Progressive motor unit loss in the G93A mouse model of amyotrophic lateral sclerosis is unaffected by gender. Muscle Nerve, 2009 39(3): p. 318–27. [PubMed: 19208415]
23. Hegedus J, et al., Preferential motor unit loss in the SOD1 G93A transgenic mouse model of amyotrophic lateral sclerosis. J Physiol, 2008 586(14): p. 3337–51. [PubMed: 18467368]
24. Shefner JM, et al., Effect of neurophilin ligands on motor units in mice with SOD1 ALS mutations. Neurology, 2001 57(10): p. 1857–61. [PubMed: 11723276]
25. Shefner JM, Cudkowicz ME, and Brown RH, Jr., Comparison of incremental with multipoint MUNE methods in transgenic ALS mice. Muscle Nerve, 2002 25(1): p. 39–42. [PubMed: 11754183]
26. Shefner JM, Cudkowicz M, and Brown RH, Jr., Motor unit number estimation predicts disease onset and survival in a transgenic mouse model of amyotrophic lateral sclerosis. Muscle Nerve, 2006 34(5): p. 603–7. [PubMed: 16892429]
27. Zhou C, et al., A method comparison in monitoring disease progression of G93A mouse model of ALS. Amyotroph Lateral Scler, 2007 8(6): p. 366–72. [PubMed: 17852023]
28. Mancuso R, et al., Electrophysiological analysis of a murine model of motoneuron disease. Clin Neurophysiol, 2011 122(8): p. 1660–70. [PubMed: 21354365]
29. Ngo ST, et al., The relationship between Bayesian motor unit number estimation and histological measurements of motor neurons in wild-type and SOD1(G93A) mice. Clin Neurophysiol, 2012 123(10): p. 2080–91. [PubMed: 22521362]
30. Li J, Sung M, and Rutkove SB, Electrophysiologic biomarkers for assessing disease progression and the effect of riluzole in SOD1 G93A ALS mice. PLoS One, 2013 8(6): p. e65976. [PubMed: 23762454]
31. Li J, et al., Single and modeled multifrequency electrical impedance myography parameters and their relationship to force production in the ALS SOD1G93A mouse. Amyotroph Lateral Scler Frontotemporal Degener, 2016 17(5–6): p. 397–403. [PubMed: 27077943]
32. Mancuso R, Osta R, and Navarro X, Presymptomatic electrophysiological tests predict clinical onset and survival in SOD1(G93A) ALS mice. Muscle Nerve, 2014 50(6): p. 943–9. [PubMed: 24619579]
33. Srivastava AK, et al., Mutant HSPB1 overexpression in neurons is sufficient to cause age-related motor neuronopathy in mice. Neurobiol Dis, 2012 47(2): p. 163–73. [PubMed: 22521462]
34. Arnold W, et al., The neuromuscular impact of symptomatic SMN restoration in a mouse model of spinal muscular atrophy. Neurobiol Dis, 2016 87: p. 116–23. [PubMed: 26733414]
35. Arnold WD, et al., Electrophysiological Biomarkers in Spinal Muscular Atrophy: Preclinical Proof of Concept. Ann Clin Transl Neurol, 2014 1(1): p. 34–44. [PubMed: 24511555]

36. Sheth KA, et al., Muscle strength and size are associated with motor unit connectivity in aged mice. Neurobiol Aging, 2018 67: p. 128–136. [PubMed: 29656012]
37. Frakes AE, et al., Additive amelioration of ALS by co-targeting independent pathogenic mechanisms. Ann Clin Transl Neurol, 2017 4(2): p. 76–86. [PubMed: 28168207]
38. Song S, et al., Major histocompatibility complex class I molecules protect motor neurons from astrocyte-induced toxicity in amyotrophic lateral sclerosis. Nat Med, 2016 22(4): p. 397–403. [PubMed: 26928464]
39. Miller TM, et al., Gene transfer demonstrates that muscle is not a primary target for non-cell-autonomous toxicity in familial amyotrophic lateral sclerosis. Proc Natl Acad Sci U S A, 2006 103(51): p. 19546–51. [PubMed: 17164329]
40. Arnold WD, et al., Electrophysiological Motor Unit Number Estimation (MUNE) Measuring Compound Muscle Action Potential (CMAP) in Mouse Hindlimb Muscles. J Vis Exp, 2015(103).
41. Gooch CL and Mosier DR, Stimulated single fiber electromyography in the mouse: techniques and normative data. Muscle Nerve, 2001 24(7): p. 941–5. [PubMed: 11410922]
42. Chai RJ, et al., Striking denervation of neuromuscular junctions without lumbar motoneuron loss in geriatric mouse muscle. PLoS One, 2011 6(12): p. e28090. [PubMed: 22164231]
43. Cheng A, et al., Sequence of age-associated changes to the mouse neuromuscular junction and the protective effects of voluntary exercise. PLoS One, 2013 8(7): p. e67970. [PubMed: 23844140]
44. Koo TK and Li MY, A Guideline of Selecting and Reporting Intraclass Correlation Coefficients for Reliability Research. J Chiropr Med, 2016 15(2): p. 155–63. [PubMed: 27330520]
45. Foust KD, et al., Therapeutic AAV9-mediated suppression of mutant SOD1 slows disease progression and extends survival in models of inherited ALS. Mol Ther, 2013 21(12): p. 2148–59. [PubMed: 24008656]
46. Holm S, A Simple Sequentially Rejective Multiple Test Procedure. Scandinavian Journal of Statistics, 1979 6(2): p. 65–70.
47. Mukaka MM, Statistics corner: A guide to appropriate use of correlation coefficient in medical research. Malawi Med J, 2012 24(3): p. 69–71. [PubMed: 23638278]
48. Chiu AY, et al., Age-dependent penetrance of disease in a transgenic mouse model of familial amyotrophic lateral sclerosis. Mol Cell Neurosci, 1995 6(4): p. 349–62. [PubMed: 8846004]
49. Pun S, et al., Selective vulnerability and pruning of phasic motoneuron axons in motoneuron disease alleviated by CNTF. Nat Neurosci, 2006 9(3): p. 408–19. [PubMed: 16474388]
50. Johnson MA, et al., A comparison of fibre size, fibre type constitution and spatial fibre type distribution in normal human muscle and in muscle from cases of spinal muscular atrophy and from other neuromuscular disorders. J Neurol Sci, 1973 20(4): p. 345–61. [PubMed: 4272515]
51. Luo G, et al., Defective mitochondrial dynamics is an early event in skeletal muscle of an amyotrophic lateral sclerosis mouse model. PLoS One, 2013 8(12): p. e82112. [PubMed: 24324755]
52. Watanabe H, et al., A rapid functional decline type of amyotrophic lateral sclerosis is linked to low expression of TTN. J Neurol Neurosurg Psychiatry, 2016 87(8): p. 851–8. [PubMed: 26746183]
53. Yi J, et al., Mitochondrial calcium uptake regulates rapid calcium transients in skeletal muscle during excitation-contraction (E-C) coupling. J Biol Chem, 2011 286(37): p. 32436–43. [PubMed: 21795684]
54. Dobrowolny G, et al., Skeletal muscle is a primary target of SOD1G93A-mediated toxicity. Cell Metab, 2008 8(5): p. 425–36. [PubMed: 19046573]
55. Yamada T, et al., Oxidation of myosin heavy chain and reduction in force production in hyperthyroid rat soleus. J Appl Physiol (1985), 2006 100(5): p. 1520–6. [PubMed: 16397059]
56. Powers SK, et al., Reactive oxygen species: impact on skeletal muscle. Compr Physiol, 2011 1(2): p. 941–69. [PubMed: 23737208]
57. Arai M, et al., Mechanism of doxorubicin-induced inhibition of sarcoplasmic reticulum Ca(2+)-ATPase gene transcription. Circ Res, 2000 86(1): p. 8–14. [PubMed: 10625299]
58. Qaisar R, et al., Oxidative stress-induced dysregulation of excitation-contraction coupling contributes to muscle weakness. J Cachexia Sarcopenia Muscle, 2018.

59. Heiman-Patterson TD, et al., Background and gender effects on survival in the TgN(SOD1-G93A)1Gur mouse model of ALS. J Neurol Sci, 2005 236(1–2): p. 1–7. [PubMed: 16024047]

60. Veldink JH, et al., Sexual differences in onset of disease and response to exercise in a transgenic model of ALS. Neuromuscul Disord, 2003 13(9): p. 737–43. [PubMed: 14561497]

61. Bowser R, Turner MR, and Shefner J, Biomarkers in amyotrophic lateral sclerosis: opportunities and limitations. Nat Rev Neurol, 2011 7(11): p. 631–8. [PubMed: 21989244]

62. Ives CT and Doherty TJ, Intra- and inter-rater reliability of motor unit number estimation and quantitative motor unit analysis in the upper trapezius. Clin Neurophysiol, 2012 123(1): p. 200–5. [PubMed: 21683650]

63. Ives CT and Doherty TJ, Intra-rater reliability of motor unit number estimation and quantitative motor unit analysis in subjects with amyotrophic lateral sclerosis. Clin Neurophysiol, 2014 125(1): p. 170–8. [PubMed: 23867065]

64. Neuwirth C, et al., Motor Unit Number Index (MUNIX): a novel neurophysiological marker for neuromuscular disorders; test-retest reliability in healthy volunteers. Clin Neurophysiol, 2011 122(9): p. 1867–72. [PubMed: 21396884]

65. Clark BC, Cook SB, and Ploutz-Snyder LL, Reliability of techniques to assess human neuromuscular function in vivo. J Electromyogr Kinesiol, 2007 17(1): p. 90–101. [PubMed: 16427317]

66. Kaya RD, Hoffman RL, and Clark BC, Reliability of a modified motor unit number index (MUNIX) technique. J Electromyogr Kinesiol, 2014 24(1): p. 18–24. [PubMed: 24168818]

67. Sleivert GG and Wenger HA, Reliability of measuring isometric and isokinetic peak torque, rate of torque development, integrated electromyography, and tibial nerve conduction velocity. Arch Phys Med Rehabil, 1994 75(12): p. 1315–21. [PubMed: 7993170]

68. Kasselman LJ, Shefner JM, and Rutkove SB, Motor unit number estimation in the rat tail using a modified multipoint stimulation technique. Muscle Nerve, 2009 40(1): p. 115–21. [PubMed: 19533644]

69. Beck M, et al., Comparison of maximal voluntary isometric contraction and Drachman's hand-held dynamometry in evaluating patients with amyotrophic lateral sclerosis. Muscle Nerve, 1999 22(9): p. 1265–70. [PubMed: 10454724]

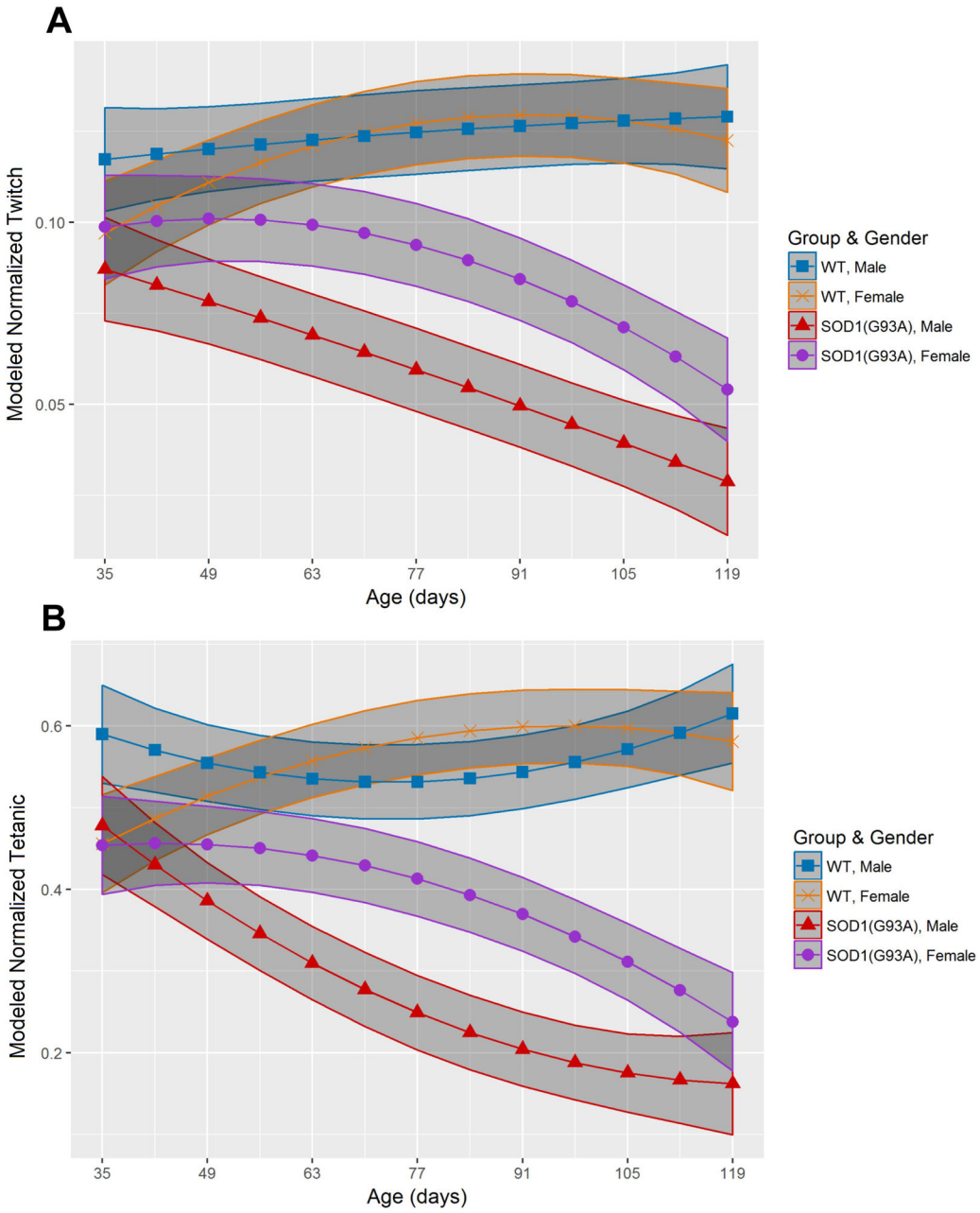

Figure 1.

SOD1(G93A) males demonstrate earlier muscle contractility reduction than SOD1(G93A) females. (A) Modeled twitch torque (normalized to body mass) (mN-m/g) outcomes of wildtype (WT) male mice (blue square, n=5), wildtype female mice (orange x, n=5), SOD1(G93A) male mice (red triangle, n=5) and SOD1 female mice (purple circle, n=5). (B) Modeled tetanic torque (normalized to body mass) (mN-m/g) outcomes in wildtype and SOD1(G93A) cohorts, organized by gender. Shaded regions depict 95% confidence interval.

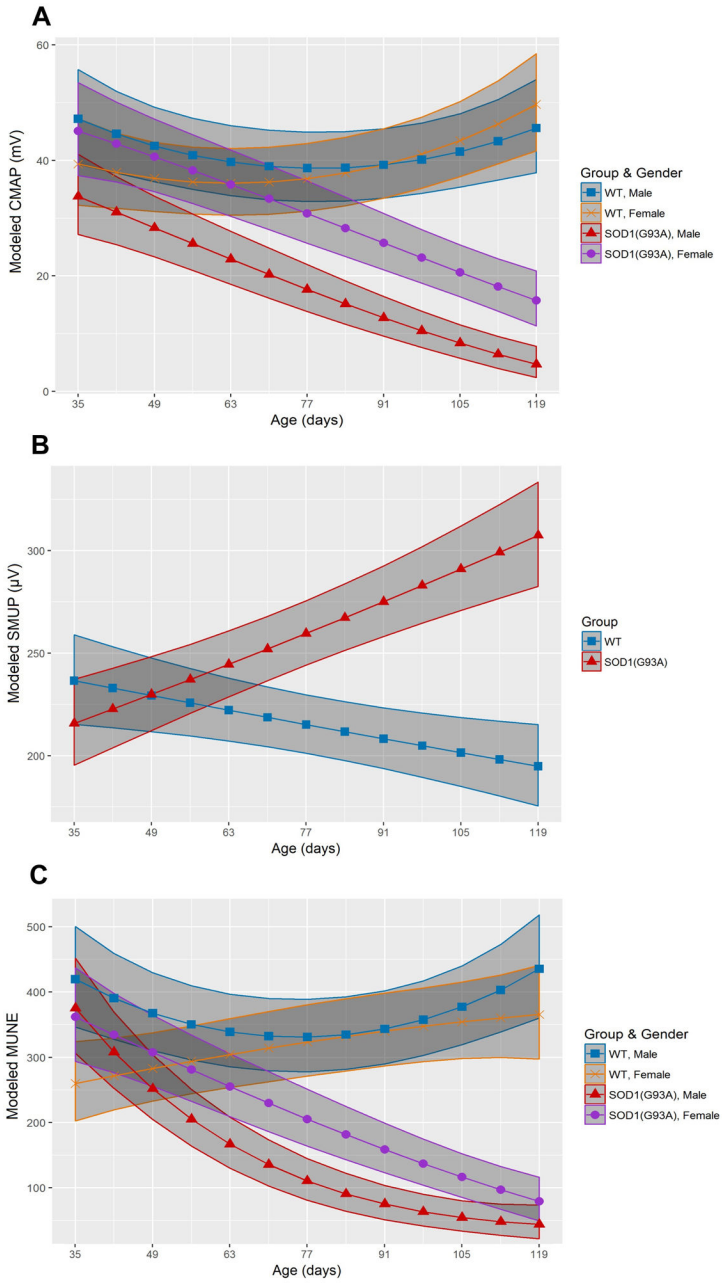

Figure 2.

SOD1(G93A) males demonstrate earlier MU connectivity reduction than SOD1(G93A) females. (A) Longitudinal modeled CMAP (mV) of wildtype male mice (blue square, n=5), wildtype female mice (orange x, n=5), SOD1(G93A) male mice (red triangle, n=5) and SOD1 female mice (purple circle, n=5). (B) Modeled SMUP (μV) of wildtype mice (blue square, n=10) and SOD1(G93A) mutants (red triangle, n=10). (C) Modeled MUNE of wildtype male mice, wildtype female mice, SOD1(G93A) male mice and SOD1(G93A) female mice. Shaded regions depict 95% confidence interval. Abbreviations: compound muscle action potential (CMAP), single motor unit potential (SMUP), motor unit number estimation (MUNE), and wildtype (WT).

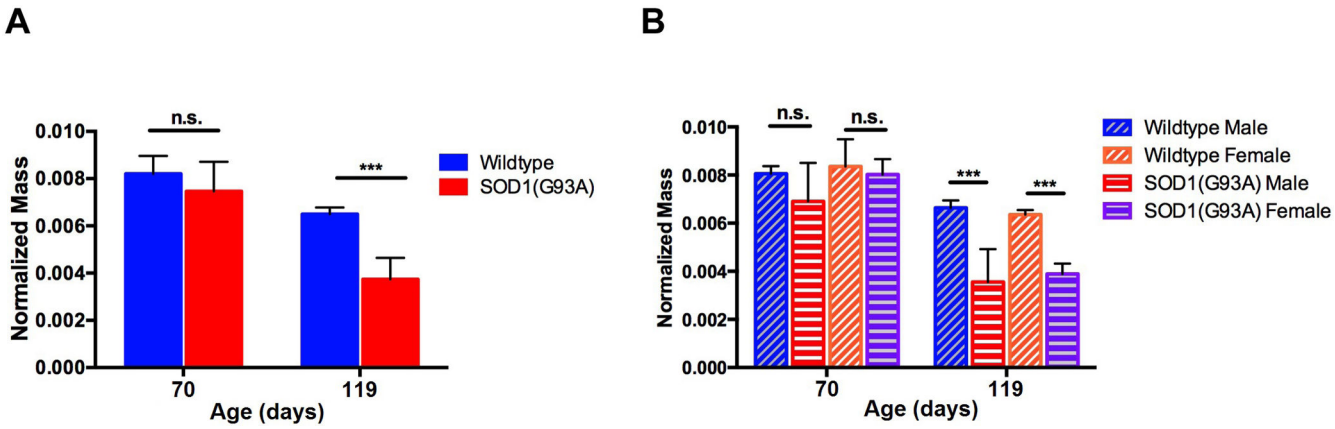

Figure 3.

Normalized triceps surae wet mass at P70 and P119. (A) Normalized triceps surae mass at P70 (wildtype: 0.0082g±0.0008g, n=6 vs SOD1(G93A): 0.0075g±0.00130g, n=6; p=0.123) and P119 (wildtype: 0.0065g±0.0003g, n=10 vs SOD1(G93A): 0.0037g±0.0009g, n=9). (B) Normalized triceps surae wet mass by gender at P70 (wildtype males: 0.0081g±0.0003g, n=3 vs SOD1(G93A) males: 0.0069g±0.0016g n=3, p=0.19; wildtype females: 0.0084g ±0.0011g, n=3 vs SOD1(G93A) females: 0.0083g±0.0006g, n=3, p=0.52) and P119 (wildtype males: 0.0066g±0.0003g, n=5 vs SOD1(G93A) males: 0.0035g±0.0014g, n=4; wildtype females: 0.0064g±0.0002g, n=5 vs SOD1(G93A) females: 0.0039g±0.0004g, n=5). Error bars denote standard deviation. n.s.=no significance, *** = p<0.001.

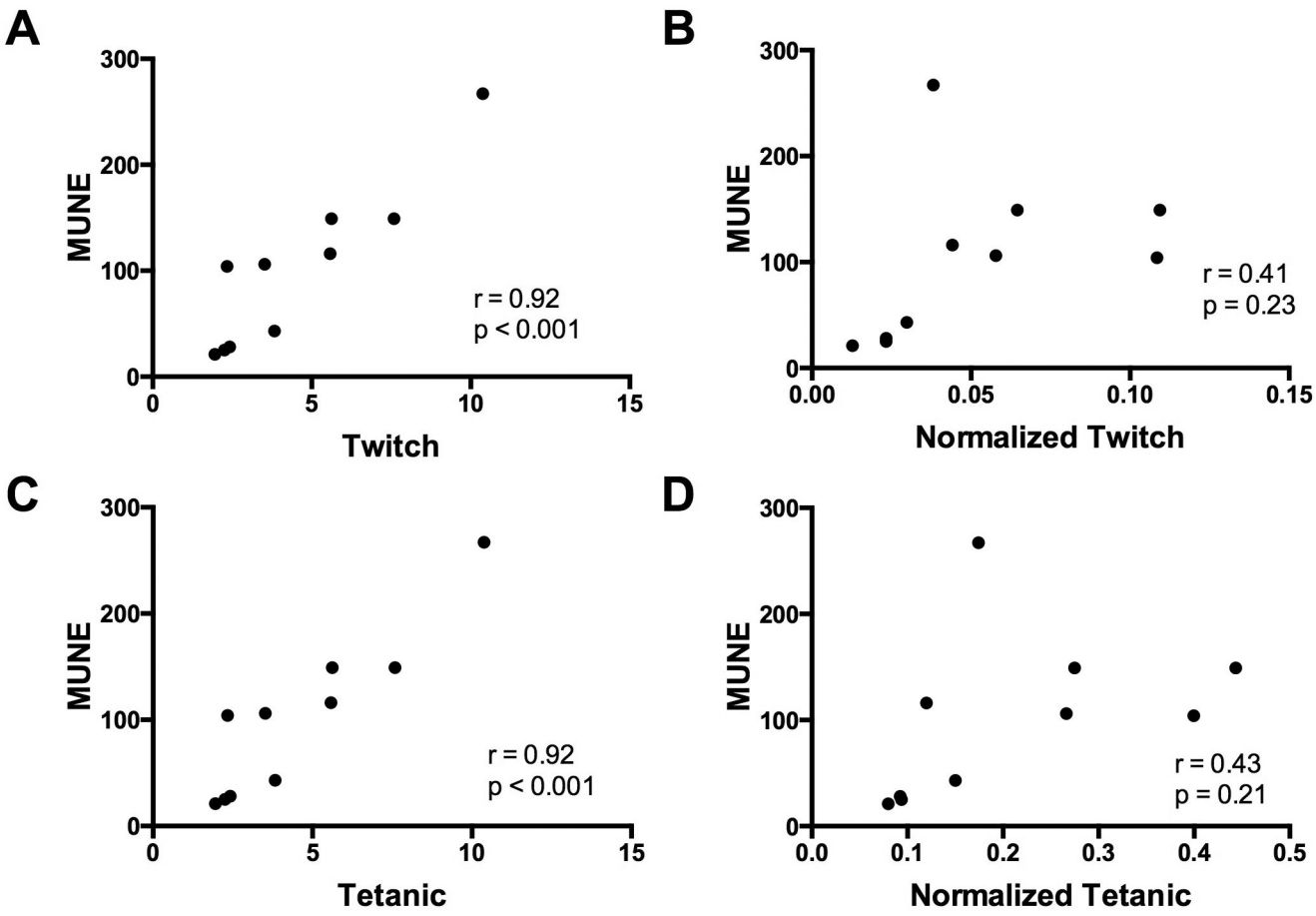

Figure 4.

Correlations of muscle contractility with MUNE. (A-B) Correlation of Motor Unit Number (MUNE) with (A) absolute twitch torque and (B) normalized twitch torque. (C-D) Correlation of MUNE with (C) absolute twitch torque and (D) normalized tetanic torque. Abbreviations: motor unit number estimation (MUNE).

Table 1

Longitudinal outcome measurements in SOD1(G93A) and wildtype male mice.

Age (PND)	CMAP (mV) (±StDv)	MUNE (±StDv)	SMUP (μV) (±StDv)	Normalized Twitch (mN-m/g) (±StDv)	Normalized Tetanic (mN-m/g) (±StDv)
35	45.0 (8.0)	383 (109)	250.4 (26.6)	0.127 (0.02)	0.59 (0.064)
	34.02 (8.3)	323 (119)	258.7 (73.2)	0.093 (0.027)	0.48 (0.12)
42	41.7 (4.7)	376 (118)	233.8 (73.3)	0.096 (0.014)	0.57 (0.089)
	30.46 (3.8)	359 (127)	184.2 (49.3)	0.083 (0.018)	0.46 (0.17)
49	46.8 (13.1)	433 (158)	208.2 (49.4)	0.123 (0.018)	0.57 (0.080)
	45.38 (5.0)	367 (70)	236.7 (46.2)	0.079 (0.011)	0.38 (0.054)
56	43.8 (6.9)	390 (47)	204.3 (34.2)	0.142 (0.016)	0.59 (0.06)
	34.28 (2.8)	317 (78)	201.2 (12.7)	0.083 (0.016)	0.34 (0.046)
63	30.0 (16.5)	239 (106)	211.8 (29.7)	0.089 (0.043)	0.40 (0.21)
	25.84 (13.9)	200 (113)	226.3 (56.1)	0.057 (0.035)	0.26 (0.15)
70	29.4 (9.1)	293 (148)	213.0 (69.9)	0.102 (0.039)	0.45 (0.21)
	23.9 (17.7)	147 (132)	318.1 (87.6)	0.074 (0.029)	0.38 (0.14)
77	31.5 (9.0)	255 (118)	230.4 (61.7)	0.146 (0.011)	0.59 (0.088)
	17.46 (15.1)	105 (81)	302.5 (68.0)	0.057 (0.034)	0.25 (0.14)
84	43.3 (11.4)	481 (150)	170.8 (51.4)	0.138 (0.012)	0.58 (0.093)
	14.2 (8.9)	105 (87)	240.2 (63.0)	0.060 (0.032)	0.21 (0.049)
91	42.3 (12.7)	390 (99)	199.9 (50.0)	0.144 (0.011)	0.59 (0.080)
	12.46 (7.3)	102 (103)	227.9 (107.8)	0.046 (0.027)	0.19 (0.12)
98	44.9 (3.6)	397 (88)	184.9 (45.8)	0.123 (0.01)	0.57 (0.036)
	11.06 (8.7)	78 (73)	291.4 (108.2)	0.037 (0.014)	0.16 (0.038)
105	49.9 (9.8)	385 (86)	249.0 (43.4)	0.135 (0.019)	0.60 (0.090)
	9.72 (10.4)	77 (107)	228.5 (55.6)	0.031 (0.020)	0.14 (0.081)
112	48.5 (9.3)	409 (100)	205.5 (75.2)	0.118 (0.01)	0.58 (0.029)
	9.95 (12.3)	59 (64)	293.0 (50.3)	0.031 (0.015)	0.17 (0.072)
119	42.1 (5.0)	407 (145)	200.1 (59.1)	0.131 (0.001)	0.60 (0.050)
	9.0 (8.4)	45 (42)	351.3 (100.0)	0.037 (0.023)	0.18 (0.074)

SOD1(G93A) male mice (shaded, n=5); wildtype male mice (unshaded, n=5). Mean outcome measurements with standard deviation (StDv) in brackets. Twitch and tetanic outcome measurements were normalized to mouse body mass. Abbreviations: Compound muscle action potential (CMAP), motor unit number estimation (MUNE), single motor unit potential (SMUP), and post-natal day (PND).

Table 2

Longitudinal outcome measurements in SOD1(G93A) and wildtype female mice.

Age (PND)	CMAP (mV) (±StDv)	MUNE (±StDv)	SMUP (μV) (±StDv)	Normalized Twitch (mN-m/g) (±StDv)	Normalized Tetanic (mN-m/g) (±StDv)
35	50.6 (9.4)	373 (75)	249.3 (50.1)	0.112 (0.005)	0.53 (0.017)
	45.8 (11.8)	387 (32)	219.7 (45.1)	0.109 (0.018)	0.50 (0.081)
42	33.4 (16.3)	262 (121)	245.7 (70.5)	0.097(0.036)	0.41 (0.17)
	38.0 (21.4)	275 (123)	233.5 (54.7)	0.079 (0.014)	0.38 (0.12)
49	41.7 (16.6)	287 (110)	253.7 (55.7)	0.113 (0.023)	0.57 (0.10)
	34.1 (12.9)	291 (173)	211.9 (43.8)	0.096 (0.031)	0.42 (0.097)
56	37.3 (14.3)	309 (108)	211.2 (26.2)	0.119 (0.020)	0.52 (0.088)
	33.5 (11.0)	236 (101)	248.8 (52.0)	0.097 (0.019)	0.44 (0.074)
63	38.4 (8.2)	291 (55)	252.5 (46.5)	0.119 (0.019)	0.51 (0.095)
	31.9 (8.3)	203 (76)	257.7 (68.1)	0.092 (0.030)	0.40 (0.081)
70	40.1 (9.0)	311 (117)	240.4 (62.9)	0.123 (0.036)	0.62 (0.11)
	34.5 (13.8)	219 (58)	256.5 (86.3)	0.102 (0.026)	0.45 (0.12)
77	44.6 (6.8)	277 (30)	260.9 (61.2)	0.127 (0.021)	0.60 (0.068)
	33.3 (10.1)	174 (77)	333.3 (90.9)	0.094 (0.013)	0.40 (0.14)
84	41.5 (6.8)	339 (141)	231.5 (67.1)	0.134 (0.014)	0.62 (0.11)
	32.0 (8.9)	196 (40)	266.4 (52.6)	0.106 (0.019)	0.47 (0.11)
91	38.5 (9.5)	407 (94)	176.53 (28.3)	0.135 (0.012)	0.58 (0.062)
	31.2 (14.9)	194 (90)	301.5 (110.6)	0.090 (0.014)	0.43 (0.079)
98	42.4 (8.8)	400 (91)	172.5 (26.3)	0.119 (0.016)	0.55 (0.059)
	21.2 (9.5)	156 (76)	264.7 (73.3)	0.081 (0.017)	0.36 (0.086)
105	39.6 (5.8)	391 (103)	178.8 (37.3)	0.119 (0.015)	0.56 (0.11)
	21.7 (8.9)	125 (23)	291.6 (77.9)	0.072 (0.034)	0.28 (0.14)
112	45.5 (14.7)	319 (35)	218.9 (48.8)	0.115 (0.010)	0.55 (0.022)
	14.7 (4.0)	83 (17)	329.8 (118.2)	0.062 (0.023)	0.26 (0.061)
119	44.9 (14.3)	347 (47)	225.0 (30.4)	0.134 (0.014)	0.64 (0.043)
	13.8 (1.9)	70 (14)	328.0 (82.9)	0.052 (0.022)	0.23 (0.081)

SOD1(G93A) female mice (shaded, n=5); wildtype female mice (unshaded, n=5). Mean outcome measurements with standard deviation (StDv) in brackets. Twitch and tetanic outcome measurements were normalized to mouse body mass. Abbreviations: Compound muscle action potential (CMAP), motor unit number estimation (MUNE), single motor unit potential (SMUP), and post-natal day (PND).

Table 3

Onset of muscle contractility and MU connectivity reduction

		Post-natal Day												
	SOD1(G93A) vs WT	**35**	**42**	**49**	**56**	**63**	**70**	**77**	**84**	**91**	**98**	**105**	**112**	**119**
Twitch	*Males*	**0.0079→**												
	Females	-	-	-	-	**0.0427→**								
Tetanic	*Males*	**0.0119→**												
	Females	-	-	-	**0.0326→**									
CMAP	*Males*	-	**0.04→**											
	Females	-	-	-	-	-	-	-	-	**0.018→**				
SMUP	*Males*	-	-	-	-	**0.0244→**								
	Females	-	-	-	-	**0.0244→**								
MUNE	*Males*	-	-	**0.0382→**										
	Females	-	-	-	-	-	-	**0.0157→**						

Abbreviations: wildtype (WT), compound muscle action potential (CMAP), single motor unit potential (SMUP), motor unit number estimation (MUNE). Dashes represent no significant difference, arrows indicate that difference was significant for duration of study.